

The results obtained in this work revealed that the glucose type aldoses react with  $[\text{Ni}(\beta\text{-ala})_2(\text{H}_2\text{O})_2]$  to yield the novel nickel(II) complexes containing the *N*-glycosides, which are the products of the first step of the "Maillard reaction".<sup>15</sup> Since the Amadori rearrangement occurs immediately after the formation of the *N*-glycosides of amino acids as the second step of the Maillard reaction and forms ketose-amino acids,<sup>6</sup> it is difficult to stop the Maillard reaction at the first step and to isolate such *N*-glycosides. Therefore it is an important fact that the Maillard reaction stopped at the first step and that the *N*-glycosides derived from amino acids and sugars can be obtained very easily by using nickel  $\beta$ -alaninato complex.

**Acknowledgment.** The authors thank Prof. Kozo Sone and Prof. Yutaka Fukuda of Ochanomizu University for obtaining magnetic data and for their helpful discussions. This work was partially supported by a Grant-in-Aid for Scientific Research from the Ministry of Education of Japan (No. 58470064).

**Registry No.** Ni(D-Glc- $\beta$ -ala)<sub>2</sub>, 99656-37-8; Ni(D-Gal- $\beta$ -ala)<sub>2</sub>, 99685-50-4; Ni(D-Xyl- $\beta$ -ala)<sub>2</sub>, 99656-38-9; Ni(D-Ribo- $\beta$ -ala)<sub>2</sub>, 99685-51-5; Ni(4,6-Bn-D-Glc- $\beta$ -ala)<sub>2</sub>, 99656-39-0; Ni( $\beta$ -ala)(H<sub>2</sub>O)(3-Me-D-Glc- $\beta$ -ala), 99656-40-3; Ni( $\beta$ -ala)<sub>2</sub>(H<sub>2</sub>O)<sub>2</sub>, 22585-11-1; D-Glc, 50-99-7; D-Gal, 59-23-4; D-Xyl, 58-86-6; D-Rib, 50-69-1; 4,6-Bn-D-Glc, 30688-66-5; 3-Me-D-Glc, 146-72-5; 2-De-D-Glc, 154-17-6.

(15) Maillard, L. C. *C. R. Hebd. Seances Acad. Sci.* **1912**, *154*, 66-68.

Contribution from the Departments of Chemistry,  
Michigan State University, East Lansing, Michigan 48824,  
and University of Virginia, Charlottesville, Virginia 22901

### Crystal and Molecular Structure of Bis[*N*-[2-(4-imidazolyl)ethyl]salicylaldiminato]iron(III) Hexafluorophosphate Ethanol Solvate: A Model for Iron(III) Sites with Tyrosine and Histidine Ligands in Proteins

J. C. Davis,<sup>1,2</sup> W.-J. Kung,<sup>1</sup> and B. A. Averill<sup>\*1,3,4</sup>

Received September 9, 1985

Iron-tyrosinate proteins<sup>5</sup> are a diverse group, including transferrin,<sup>6</sup> the catechol dioxygenases,<sup>7</sup> and the purple acid phosphatases.<sup>8</sup> The presence of tyrosine phenolate ligands to iron(III) is indicated by intense low-energy ligand to metal charge-transfer transitions; irradiation into this band gives rise to a set of resonance-enhanced Raman modes that are characteristic of coordinated phenolates. The identity of other ligands to iron is, however, more difficult to ascertain. Proton NMR studies of the purple acid phosphatases<sup>9</sup> have confirmed the presence of tyrosyl ligands to iron and have implicated histidine imidazoles as well. These conclusions have been reinforced by EXAFS studies.<sup>10</sup> A major problem in analyzing the EXAFS data of the proteins, especially the purple acid phosphatases,<sup>10c</sup> is the existence of several sets of nearest neighbors at relatively similar distances in the first shell. A lack of structurally characterized iron(III) complexes containing phenolate and imidazole ligands has made it difficult to distinguish between tyrosinate oxygens at relatively short distances and bridging oxo groups.<sup>10c</sup> Although to date no synthetic complex containing imidazole, phenolate, and bridging oxo groups has been prepared, Que et al.<sup>7a</sup> have briefly reported the preparation and resonance Raman spectrum of a mononuclear complex containing both phenolate and imidazole ligands,  $[\text{Fe}(\text{salhis})_2]\text{ClO}_4 \cdot \text{H}_2\text{O}$ .<sup>11</sup> This complex provides a convenient model for mononuclear Fe(III) sites and

\* To whom correspondence should be addressed at the University of Virginia.

**Table I.** Summary of Crystal Data and X-ray Data Collection and Reduction for  $[\text{Fe}(\text{salhis})_2]\text{PF}_6 \cdot \text{EtOH}$

Crystal Parameters	
cryst syst	orthorhombic
space group	<i>Pbca</i>
cryst habit	rectangular needle elongated along <i>c</i>
cryst dimens, mm <sup>3</sup>	0.83 × 0.09 × 0.13
<i>a</i> , Å	16.43 (1)
<i>b</i> , Å	18.21 (1)
<i>c</i> , Å	19.85 (1)
<i>V</i> , Å <sup>3</sup>	5940.6 (2)
<i>Z</i>	8
<i>d</i> (calcd), g cm <sup>-3</sup>	1.510
abs coeff, cm <sup>-1</sup>	5.814
formula	C <sub>26</sub> H <sub>30</sub> F <sub>6</sub> FeN <sub>6</sub> O <sub>3</sub> P
fw	675.38
Data Collection and Reduction <sup>13a</sup>	
diffractometer	Picker FACS-I VDOS <sup>13b</sup>
radiation	Mo K $\alpha_1$ ( $\lambda = 0.70926$ Å), graphite monochromated
temp, °C	20
scan technique	$\theta$ - $2\theta$
scan rate, deg/min	2
scan range ( $2\theta$ ), deg	1.5-50
octant collod	+ <i>h</i> , + <i>k</i> , + <i>l</i>
transmissn factor	0.976-0.962
no. of total reflcns	5822
no. of unique data with $I > 2\sigma(I)$	2160

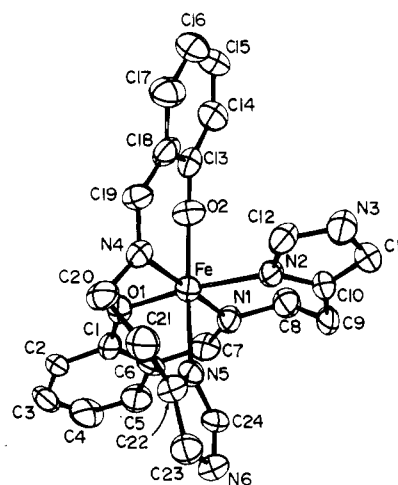


**Figure 1.** ORTEP diagram of the  $[\text{Fe}(\text{salhis})_2]^+$  cation (50% probability ellipsoids), showing the atomic numbering scheme. Hydrogen atoms have been omitted for clarity.

for comparison to bridged binuclear sites. We have now obtained crystals of the  $\text{PF}_6^-$  salt of  $[\text{Fe}(\text{salhis})_2]^+$ , and we describe herein

- (1) Michigan State University.
- (2) Current address: SOHIO Research Center, 4440 Warrensville Road, Cleveland, OH 44128.
- (3) University of Virginia.
- (4) B.A.A. was an Alfred P. Sloan Foundation Fellow, 1981-1985.
- (5) (a) Que, L., Jr. *Coord. Chem. Rev.* **1983**, *50*, 73-108. (b) Keyes, W. E.; Loehr, T. M.; Taylor, M. L. *Biochim. Biophys. Res. Commun.* **1978**, *83*, 941-945.
- (6) (a) Ainscough, E. W.; Brodie, A. M.; Plowman, J. E.; Bloor, S. J.; Loehr, J. S.; Loehr, T. M. *Biochemistry* **1980**, *19*, 4072-4079. (b) Aisen, P.; Listowsky, I. *Annu. Rev. Biochem.* **1980**, *49*, 357-393.
- (7) (a) Que, L., Jr.; Heistand, R. H., II; Mayer, R.; Roe, A. L. *Biochemistry* **1980**, *19*, 2588-2593. (b) Que, L., Jr.; Epstein, R. M. *Biochemistry* **1981**, *20*, 2545-2549. (c) Que, L., Jr. *Struct. Bonding (Berlin)* **1980**, *40*, 39-72.
- (8) (a) Antanaitis, B. C.; Aisen, P. In "Advances in Inorganic Biochemistry"; Thiel, E., Eichhorn, G., Marzilli, L., Eds.; Elsevier: Amsterdam, 1983; Vol. 5, pp 111-136. (b) Antanaitis, B. C.; Streakas, T.; Aisen, P. *J. Biol. Chem.* **1982**, *257*, 3766-3770. (c) Davis, J. C.; Averill, B. A. *Proc. Natl. Acad. Sci. U.S.A.* **1982**, *79*, 4623-4627.
- (9) (a) Lauffer, R. B.; Antanaitis, B. C.; Aisen, P.; Que, L., Jr. *J. Biol. Chem.* **1983**, *258*, 14212-14218. (b) Que, L., Jr.; Averill, B. A., unpublished results.

**Table II.** Positional Parameters and Standard Deviations (in Parentheses) in  $[\text{Fe}(\text{salhis})_2]\text{PF}_6 \cdot \text{EtOH}$ 

atom	x	y	z	atom	x	y	z
Fe	0.25779 (8)	0.31207 (7)	0.10451 (6)	F(4)	0.4097 (6)	0.1050 (6)	0.2722 (4)
O(1)	0.1575 (3)	0.3042 (4)	0.0557 (3)	F(5)	0.5162 (5)	0.1676 (5)	0.2951 (4)
O(2)	0.2151 (3)	0.3774 (3)	0.1710 (3)	F(6)	0.5034 (8)	0.0560 (5)	0.3314 (5)
N(1)	0.2863 (4)	0.4021 (4)	0.0405 (4)	H(2)	0.046 (4)	0.251 (4)	-0.014 (4)
N(2)	0.3758 (4)	0.3209 (4)	0.1491 (4)	H(3)	-0.002 (6)	0.295 (6)	-0.109 (6)
N(3)	0.4685 (6)	0.3195 (6)	0.2263 (5)	H(4)	0.075 (4)	0.377 (5)	-0.177 (4)
N(4)	0.2222 (4)	0.2242 (4)	0.1680 (4)	H(5)	0.185 (4)	0.447 (4)	-0.136 (3)
N(5)	0.3142 (4)	0.2313 (4)	0.0403 (4)	H(7)	0.257 (6)	0.456 (5)	-0.036 (4)
N(6)	0.3841 (5)	0.1835 (6)	-0.0419 (4)	H(8A)	0.341 (5)	0.476 (5)	0.099 (4)
C(1)	0.1367 (5)	0.3231 (6)	-0.0049 (5)	H(8B)	0.350 (4)	0.489 (4)	0.028 (4)
C(2)	0.0698 (6)	0.2921 (6)	-0.0368 (6)	H(9A)	0.475 (3)	0.455 (3)	0.067 (3)
C(3)	0.0441 (8)	0.3127 (9)	-0.0998 (7)	H(9B)	0.447 (5)	0.365 (5)	0.033 (4)
C(4)	0.0833 (8)	0.369 (1)	-0.1310 (7)	H(11)	0.547 (5)	0.395 (4)	0.177 (4)
C(5)	0.1502 (7)	0.4007 (6)	-0.1042 (6)	H(12)	0.367 (4)	0.253 (4)	0.225 (4)
C(6)	0.1778 (6)	0.3805 (6)	-0.0414 (5)	H(14)	0.204 (4)	0.473 (3)	0.260 (4)
C(7)	0.2471 (8)	0.4170 (5)	-0.0129 (5)	H(15)	0.202 (5)	0.468 (5)	0.376 (5)
C(8)	0.3517 (8)	0.4540 (7)	0.0600 (7)	H(16)	0.209 (4)	0.352 (5)	0.436 (5)
C(9)	0.4334 (6)	0.4174 (6)	0.0695 (6)	H(17)	0.186 (6)	0.265 (5)	0.354 (5)
C(10)	0.4368 (6)	0.3701 (5)	0.1322 (5)	H(19)	0.190 (4)	0.205 (4)	0.260 (4)
C(11)	0.4939 (7)	0.3699 (7)	0.1809 (6)	H(20A)	0.170 (4)	0.153 (3)	0.096 (3)
C(12)	0.3986 (6)	0.2915 (6)	0.2062 (6)	H(20B)	0.191 (4)	0.120 (3)	0.174 (3)
C(13)	0.2122 (5)	0.3689 (6)	0.2371 (6)	H(21A)	0.298 (4)	0.059 (5)	0.113 (4)
C(14)	0.2098 (7)	0.4320 (8)	0.2787 (7)	H(21B)	0.332 (4)	0.128 (4)	0.142 (3)
C(15)	0.2062 (7)	0.4233 (9)	0.3469 (7)	H(23)	0.382 (4)	0.073 (4)	-0.012 (4)
C(16)	0.2048 (7)	0.358 (1)	0.3779 (6)	H(24)	0.344 (5)	0.276 (4)	-0.043 (4)
C(17)	0.2070 (8)	0.294 (1)	0.3391 (7)	H(N3)	0.485 (5)	0.313 (5)	0.265 (4)
C(18)	0.2096 (5)	0.3005 (6)	0.2677 (5)	H(N6)	0.422 (4)	0.175 (4)	-0.073 (4)
C(19)	0.2078 (6)	0.2321 (6)	0.2305 (6)	O(3)	0.0171 (5)	0.3496 (5)	0.1354 (4)
C(20)	0.2122 (7)	0.1509 (6)	0.1392 (6)	C(25)	0.015 (1)	0.4274 (9)	0.1465 (9)
C(21)	0.2914 (8)	0.1205 (7)	0.1121 (7)	C(26)	0.049 (1)	0.472 (1)	0.092 (1)
C(22)	0.3244 (6)	0.1585 (7)	0.0514 (5)	H(25A)	0.045 (6)	0.436 (6)	0.176 (5)
C(23)	0.3682 (6)	0.1279 (7)	0.0020 (6)	H(25B)	-0.049 (4)	0.446 (4)	0.159 (3)
C(24)	0.3523 (7)	0.2461 (8)	-0.0167 (6)	H(26A)	0.025 (9)	0.457 (8)	0.041 (7)
P	0.4526 (2)	0.1248 (2)	0.3362 (2)	H(26B)	0.103 (6)	0.465 (5)	0.077 (5)
F(1)	0.4019 (5)	0.1948 (5)	0.3418 (4)	H(26C)	0.032 (6)	0.522 (6)	0.136 (6)
F(2)	0.4983 (5)	0.1478 (6)	0.4009 (4)	H(O3)	0.058 (5)	0.338 (5)	0.121 (4)
F(3)	0.3929 (6)	0.0864 (5)	0.3841 (5)				

**Table III.** Selected Interatomic Distances (Å) and Angles (deg) in  $[\text{Fe}(\text{salhis})_2]\text{PF}_6 \cdot \text{EtOH}$ 

Distances			
Fe-O(1)	1.917 (6)	Fe-N(2)	2.138 (7)
Fe-O(2)	1.910 (6)	Fe-N(4)	2.119 (8)
Fe-N(1)	2.127 (8)	Fe-N(5)	2.156 (7)
Angles			
O(1)-Fe-O(2)	94.6 (3)	N(1)-Fe-N(2)	89.4 (4)
O(1)-Fe-N(1)	86.9 (3)	N(1)-Fe-N(4)	176.7 (4)
O(1)-Fe-N(2)	174.1 (4)	N(1)-Fe-N(5)	94.4 (4)
O(1)-Fe-N(4)	90.4 (3)	N(2)-Fe-N(4)	93.5 (4)
O(1)-Fe-N(5)	91.1 (3)	N(2)-Fe-N(5)	84.6 (3)
O(2)-Fe-N(1)	90.8 (3)	N(4)-Fe-N(5)	87.5 (4)
O(2)-Fe-N(2)	90.0 (3)	Fe-O(1)-C(1)	132.5 (4)
O(2)-Fe-N(4)	87.6 (4)	Fe-O(2)-C(13)	128.7 (5)
O(2)-Fe-N(5)	172.5 (4)		

its structure. This constitutes the first structurally characterized high-spin iron(III) complex containing both imidazole and phenolate ligands.

### Experimental Section

**Materials.** Histamine, ammonium hexafluorophosphate, and salicylaldehyde (as the bisulfite) were obtained from Sigma, Alfa, and Eastman, respectively.  $[\text{Fe}(\text{salhis})_2]\text{PF}_6$  was prepared as described,<sup>7a</sup> except that anhydrous  $\text{FeCl}_3$  (0.75 g) was substituted for ferrous perchlorate

hexahydrate (1.68 g). The resulting solution of  $[\text{Fe}(\text{salhis})_2]^+$  in MeOH was treated with  $(\text{NH}_4)(\text{PF}_6)$  (0.49 g, 4.6 mmol), yielding a purple precipitate that was filtered, washed with  $\text{Et}_2\text{O}$ , and dried. Crystallization from absolute EtOH by slow cooling to  $-20^\circ\text{C}$  gave purple crystals of the EtOH solvate.<sup>12</sup> Anal. Calcd for  $\text{C}_{26}\text{H}_{30}\text{F}_6\text{FeN}_6\text{O}_3\text{P}$ : C, 46.26; H, 4.49; F, 16.89; Fe, 8.44; N, 12.45; P, 4.59. Found: C, 45.58; H, 4.42; F, 16.94; Fe, 8.44; N, 12.39; P, 4.59.

**X-ray Structure Determination.** Details of crystal data and X-ray diffraction data collection are given in Table I. The data were corrected for Lorentz, polarization, and background effects and for absorption. Observed extinctions ( $h00$ ,  $h \neq 2n$ ;  $0kl$ ,  $k \neq 2n$ ;  $h0l$ ,  $l \neq 2n$ ;  $h00$ ,  $h \neq 2n$ ;  $0k0$ ,  $k \neq 2n$ ;  $00l$ ,  $l \neq 2n$ ) were consistent with space group  $Pbca$ . No decay of the intensity of standard reflections was noted.

The structure was solved by the Patterson method. Full-matrix least-squares refinement<sup>13c-f</sup> and difference-Fourier calculations were used to locate all remaining non-hydrogen atoms; hydrogen atoms were inserted at calculated positions and subsequently refined isotropically.

(12)  $\lambda_{\text{max}}(\text{MeCN}) = 535 \text{ nm}$ ;  $\epsilon(\text{MeCN}) = 3800 \text{ M}^{-1} \text{ cm}^{-1}$ ;  $\mu_{\text{eff}} = 6.0 \pm 0.1 \mu_{\text{B}}$  (4.2–300 K).

(13) (a) The X-ray diffraction intensity data were reduced (Wei, K.-T.; Ward, D. L. *Acta Crystallogr., Sect. B: Struct. Crystallogr. Cryst. Chem.* **1976**, *B32*, 2768) ( $P = 0.2$ ,  $Q = 0$ ) and their standard deviations calculated on the basis of counting statistics. An absorption correction was applied (Templeton, L. K.; Templeton, D. H. American Crystallographic Association Program and Abstracts, 1973; Series 2, Vol. 1, p 143). (b) Lenhart, P. G. *J. Appl. Crystallogr.* **1975**, *8*, 568. (c) Atomic scattering factors for all non-hydrogen atoms are from: Doyle, P. A.; Turner, P. S. *Acta Crystallogr., Sect. A: Cryst. Phys., Diffraction, Theor. Gen. Chem.* **1968**, *A24*, 390. Those for hydrogen atoms are from: Stewart, R. F.; Davidson, E. R.; Simpson, W. T. *J. Chem. Phys.* **1965**, *42*, 3175. The anomalous scattering factors are from: Cromer, D. T.; Liberman, D. *J. Chem. Phys.* **1970**, *53*, 1891. (d) All least-squares refinements were based on the minimization of  $\sum w_i |F_o| - |F_c|$  with the individual  $w_i = 1/\sigma(F_o)^2$ . (e)  $R = [\sum |F_o| - |F_c|] / \sum |F_o|$ . (f) All calculations were performed on a CDC Cyber 170 Model 750 computer using a variety of programs that have evolved from, or been assimilated into, the system of Allan Zalkin (Lawrence Berkeley Laboratory, private communication (1974)). Other programs used include ORTEP by: Johnson, C. K. *Oak Ridge Natl. Lab., [Rep.] ORNL (U.S.)* **1965**, *ORNL-3794*.

- (10) (a) Felton, R. H.; Barrow, W. L.; May, S. W.; Sowell, A. L.; Goels, S.; Bunker, G.; Stern, E. A. *J. Am. Chem. Soc.* **1982**, *104*, 6132–6134. (b) Schneider, D. J.; Roe, A. L.; Mayer, R. J.; Que, L., Jr. *J. Biol. Chem.* **1984**, *259*, 9699–9703. (c) Kauzlarich, S. M.; Teo, B. K.; Zirino, T.; Burman, S.; Davis, J. C.; Averill, B. A., submitted for publication.
- (11) Abbreviations used: salhis,  $N$ -[2-(4-imidazolyl)ethyl]salicylaldehyde monoanion; salen,  $N,N'$ -ethylenebis(salicylaldehyde) dianion; saloph,  $N,N'$ -1,2-phenylenebis(salicylaldehyde) dianion; hq, 1,4-benzenediolate; catH<sub>2</sub>, catechol; EHPG,  $N,N'$ -ethylenebis(*o*-hydroxyphenyl)glycine tetraanion.

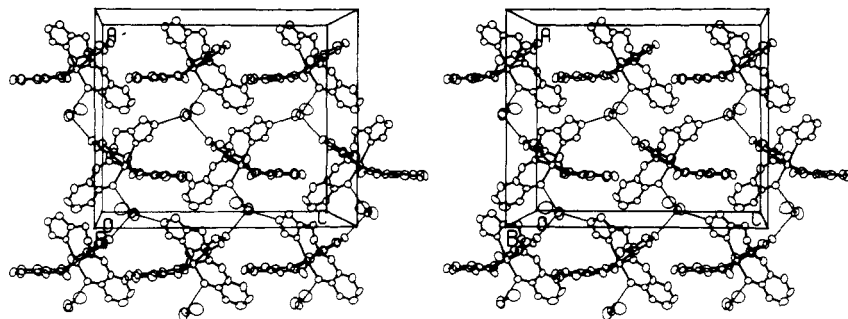


**Figure 2.** Stereoview of the unit cell of  $[\text{Fe}(\text{salhis})_2]\text{PF}_6 \cdot \text{EtOH}$ , illustrating the hydrogen-bonded layers of cations and solvent. The  $\text{PF}_6^-$  anions have been omitted for clarity.

The refinement converged at a conventional  $R$  value<sup>13e</sup> of 0.072. The final difference-Fourier map showed no peaks greater than  $0.53 \text{ e}/\text{\AA}^3$ . Final atomic coordinates are given in Table II, while a drawing of the cation illustrating the numbering system is given in Figure 1. Tables of thermal parameters and calculated and observed structure factors are given in the supplementary material.

### Results and Discussion

The crystal structure of  $[\text{Fe}(\text{salhis})_2]\text{PF}_6 \cdot \text{EtOH}$  consists of 8 cations, 8 anions, and 8 solvent molecules per unit cell. The  $\text{PF}_6^-$  anions exhibit some rotational disorder, as evidenced by relatively large anisotropic thermal parameters for the F atoms. Each EtOH of solvation is hydrogen-bonded to three complex cations via two imidazole NH's (N(3) and N(6)) and a phenoxide oxygen (O(1)). This results in layers of  $[\text{Fe}(\text{salhis})_2]^+$  cations, linked by EtOH molecules in the  $a$ - $c$  plane (Figure 2) and by  $\text{PF}_6^-$  anions in the  $b$  direction. Each EtOH oxygen atom thus achieves an "ice-like" tetrahedral H-bonded environment.

The  $[\text{Fe}(\text{salhis})_2]^+$  cations exhibit a distorted octahedral  $\text{FeN}_4\text{O}_2$  coordination geometry, with the salhis<sup>-</sup> ligands arranged in a meridional fashion (Figure 1). This results in the phenoxide oxygens being cis to one another and each being trans to an imidazole group from the same ligand. The two imine nitrogens are therefore trans. Significant distances and angles are given in Table III, while a complete listing of distances and angles and tables of least-squares planes are available in the supplementary material.

The planarity of the salicylaldimine units (C(1)-C(8) and N(1), C(13)-C(20) and N(4); greatest deviation  $\leq 0.1 \text{ \AA}$ ) results in steric constraints that preclude a facial arrangement of the tridentate ligands and accounts for the observed geometry of the complex. The O(1)-Fe-N(2) and O(2)-Fe-N(5) angles are significantly less than  $180^\circ$ , again due to steric constraints of the ligands. The rest of the angles at Fe deviate from those expected for octahedral geometry by  $\leq 4.6^\circ$ .

Of greatest importance for comparison with EXAFS results on iron proteins are the Fe-O(phenolate) and Fe-N(imidazole) distances, which average 1.914 and 2.147  $\text{\AA}$ , respectively. These results reinforce the trend of relatively short ( $\leq 1.92 \text{ \AA}$ ) phenolate bonds to Fe(III) observed in  $\text{Fe}(\text{saloph})\text{CatH}^{11}$  (average 1.905  $\text{\AA}$ ),<sup>14</sup>  $[\text{Fe}(\text{salen})]_2\text{hq}^{11}$  (average 1.905  $\text{\AA}$ ),<sup>14</sup> and  $\text{NaFe}(\text{meso-EHPG})^{11}$  (average 1.907  $\text{\AA}$ );<sup>15</sup> they also indicate that Fe(III)-N(imidazole) bond lengths (average 2.147  $\text{\AA}$ ) are similar to those observed for Fe-N(pyrazole) bonds (e.g., average 2.165  $\text{\AA}$  in  $[\text{Fe}(\text{HB}(\text{pz})_3)(\text{O}_2\text{CCH}_3)_2\text{O}]^{16}$ ) and Fe-N(imine) bonds (average 2.123  $\text{\AA}$  in  $[\text{Fe}(\text{salhis})_2]^+$ , average 2.097  $\text{\AA}$  in  $\text{Fe}(\text{saloph})\text{CatH}$ ,<sup>14</sup> and 2.096  $\text{\AA}$  in  $[\text{Fe}(\text{salen})]_2\text{hq}^{14}$ ). These distances are comparable to those observed by EXAFS for the first-shell scatterers around Fe in the catechol dioxygenases,<sup>10a</sup> transferrin,<sup>10b</sup> and the purple acid phosphatase from beef spleen.<sup>10c</sup> Also of note is the minimal effect of hydrogen bonding to O(1) on the Fe-O bond length,

which is the same for O(1) and O(2) within experimental error.

**Acknowledgment.** This research was supported by grants from the National Institutes of Health to B.A.A. (GM 28636 and GM 32117). We thank D. Ward for assistance with the X-ray structure determination.

**Registry No.**  $[\text{Fe}(\text{salhis})_2]\text{PF}_6 \cdot \text{EtOH}$ , 99684-95-4.

**Supplementary Material Available:** Complete listings of interatomic distances and angles, thermal parameters, calculated and observed structure factors, and least-squares planes (60 pages). Ordering information is given on any current masthead page.

Contribution from the Departments of Chemistry,  
University of Texas at El Paso, El Paso, Texas 79968,  
and Texas Tech University, Lubbock, Texas 79409

### pH-Dependent Metal Ion Selectivity by a Crown Ether Carboxylic Acid

C. Allen Chang,\*† Jen Twu,† and Richard A. Bartsch‡

Received May 14, 1985

The discovery of neutral cyclic polyethers, crown ethers, was followed by numerous studies in which these compounds were used in the development of ion-selective reagents, biological transport of ions across membranes, phase-transfer catalysis, and a number of other potential analytical and pharmaceutical applications. The intrinsic selectivities of these crown ethers toward metal ions have been attributed to the matching of their cavity sizes and metal ion diameters. Thus, 14-crown-4 is good for  $\text{Li}^{+1}$  and 18-crown-6 for  $\text{K}^{+2,3}$ . More intensive investigations have revealed that the simple "cavity-size" selectivity concept is not always applicable but is most useful for inflexible homologous systems.

Making structural variations within crown ethers has proven to be a valid technique for producing better ion-selective reagents. The variations include changing the type and the number of donor atoms, adding pendent coordinating groups, and preparing more elaborate macropolycyclic compounds. For example, Gokel et al. prepared several lariat crowns (i.e. crown ethers with neutral binding sites on pendent sidearms) and found that formation constants of their metal complexes are higher than those without sidearms. Presumably this is due to sidearm participation in complexation.<sup>4</sup> It was also found that N-pivot lariat crowns are more flexible and form stronger complexes than C-pivot lariat crowns if the other structures are otherwise similar.<sup>5</sup> On the other hand, if the pendent group has a negative charge, Coulombic interaction between the ligand and metal ion and the resulting charge neutralization provide even stronger complexation; e.g., the formation constant for  $\text{Na}^{+}$  complexation by the radical anion form of *N*-(2-nitrobenzyl)monoaza-15-crown-5 is 25 000 times

(14) Heistand, R. H., II; Roe, A. L.; Que, L., Jr. *Inorg. Chem.* **1982**, *21*, 676-681.

(15) Bailey, N. A.; Cummins, D.; McKenzie, E. D.; Worthington, J. M. *Inorg. Chim. Acta* **1981**, *50*, 111-120.

(16) Armstrong, W. H.; Spool, A.; Papaefthymion, G. C.; Frankel, R. B.; Lippard, S. J. *J. Am. Chem. Soc.* **1984**, *106*, 3653-3667.

\*University of Texas at El Paso.

†Texas Tech University.